EXPERIMENTAL VISUALIZATION OF THE FLOW INSIDE OPEN CAVITIES

Eduardo F. Mega, **eduardomega@dem.feis.unesp.br**
Vinicius S. Morais, **vvinicius@dem.feis.unesp.br**
Edson D. R. Vieira, **delrio@dem.feis.unesp.br**
Sérgio S. Mansur, **mansur@dem.feis.unesp.br**
UNESP Ilha Solteira – Mechanical Engineering Department, Av. Brasil 56, ZIP Code 15385-000, Ilha Solteira, SP, Brazil

Abstract. *In the present paper, flow inside open cavities has been experimentally studied for different aspect ratios and Reynolds numbers up to 1300. Flow visualizations tests have been performed in a free surface water channel using two distinct techniques – liquid dye injection and solid micro-particles suspended in the water. Images have been captured by means of a still digital camera with several exposure times. Experimental results have shown that the use of solid tracers is very adequate for the visualization of stationary eddy structures. However, the use of that technique does not allow identifying Kelvin-Helmholtz instabilities usually formed in the shear region above the cavity. Flow patterns obtained in this work have been compared with visual results from other authors and a good agreement has been reached.*

Keywords*: open cavity, flow visualization, dye injection, solid tracers.*

1. INTRODUCTION

The flow inside open cavities is a classical problem in fluid mechanics, which presents great practical interest. In atmospheric sciences, that kind of flow arise many situations, e.g., urban canyons, small valleys and hollows. In engineering applications, cavity flow is frequently found in opened gaps on external walls and fairing of terrestrial vehicles, wings and fuselages of airplanes, and shells of watercrafts, as well as over aerial or oceanic structures submitted to wind action or water motion. In such a flow vortex-shedding mechanism and vortex-wall interaction can cause drag increasing, erosion, noise, and premature failure in machines and equipments.

Flow past open cavities has been investigated by several authors for more than a half-century. The most works about that subject focuses on compressible flows – such as Colonius *et al.* (1999a,b), Henderson *et al.* (2001), Ludovic *et al.* (2002), Gloerfelt *et al.* (2002), Gloerfelt *et al.* (2003a,b), Hamed *et al.* (2003), and Samimy *et al.* (2003) – and are concerned with controlling resonant instabilities and noise produced by aerodynamically induced pressure oscillations. The current available information on incompressible flow inside cavities is sharply smaller.

Shen and Floryan (1985) have numerically studied the incompressible flow in two-dimensional cavities with aspect ratio from 0.5 to 4 at very low Reynolds number, about 0.01. The results obtained by the authors have been confronted with available experimental data from the literature, presenting a good agreement.

Sinha *et al.* (1982) have experimentally investigated the flow within rectangular cavities with aspect ratio varying from 0.035 to 2.5, at three different values of Reynolds number – Re = 662, 1342, and 2648. That work has provided a useful database to validate numerical simulation codes and, for that reason, has become one of the main references about the subject for a long time.

Using laser Doppler velocimetry, Esteve *et al.* (2000) and Reulet *et al.* (2002) have studied the flow past a cavity with aspect ratio of 10, for Reynolds numbers 3.8×10^4 and 6.4×10^4. The flow field has been described in terms of velocity vectors and turbulence intensity, providing insight on the basic physics underlying the fluid dynamics behavior of large cavities at moderate Reynolds number.

In order to improve heat transfer process in solar collectors, Zdansky *et al.* (2000, 2001, 2003) have numerically simulated two-dimensional incompressible flows in open cavities. A wide range of Reynolds number has been considered by the investigators, including laminar and turbulent flows. In those latter computations a k-ε model has been employed for unsteady RANS closure.

Similar calculations have been carried out by Kim *et al.* (2001) in an investigation directed to pollutant dispersion in urban canyons. The unsteady flow past two buildings in side-by-side arrangement and a hill followed by two buildings downstream have been studied. The authors have shown that the flow patterns and the pollutant concentration depend strongly on the aspect ratio of the cavities.

In a relatively recent work, Arruda (2004) has used the open cavity problem as a benchmark for testing a new immersed boundary formulation previously proposed by Lima e Silva *et al.* (2003). For validating numerical approach, calculated results have been compared with experimental data of Sinha *et al.* (1982).

The present paper concerns with an experimental investigation on the flow inside open cavities with different aspect ratios. Flow visualizations have been performed at different Reynolds numbers using two distinct classical techniques – liquid dye injection and solid micro-particles mixed in the water flow. Flow patterns are analyzed and compared with numerical results from other authors.

2. EXPERIMENTAL APPARATUS AND PROCEDURE

All experimental runs have been conducted in a free-surface closed-circuit water channel, specially designed and constructed within the present project. In a brief description, this apparatus consist of a two reservoirs (*R1* and *R2*), centrifugal pump (*CP*), flow control valve (*FC*), contraction section (*CS*), and test section (*TS*), as indicated in Fig. 1. A horizontal perforated plate (*PP*) is placed above the intake pipe (*IP*) in order to damp disturbances and to homogenize the vertical ascending flow inside reservoir *R1*. After several preliminary tests, two screens (*S1* and *S2*) have been placed at both contraction extremities for providing uniform stable flow in the test section.

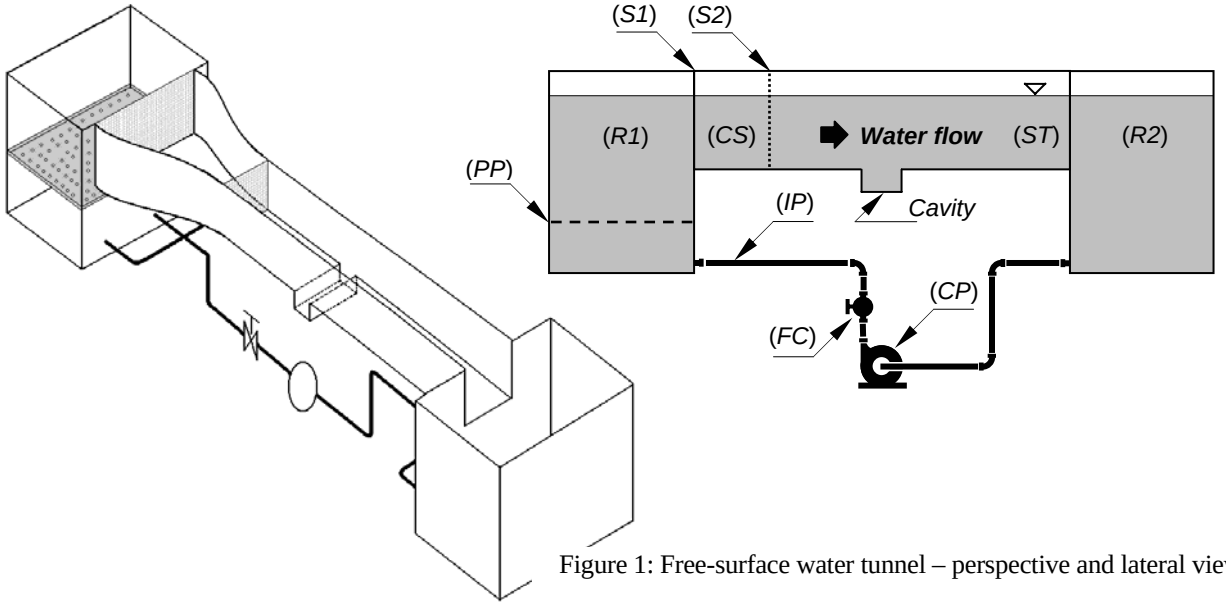

Figure 1: Free-surface water tunnel – perspective and lateral view.

The test section is built in transparent Plexiglas™ and has a rectangular transverse section with nominal size of 140 x 190 x 600 mm. The cavity, positioned in the bottom surface of the test section, is interchanging and can be easily replaced. The main geometrical parameters that define a cavity are presented in Fig. 2.

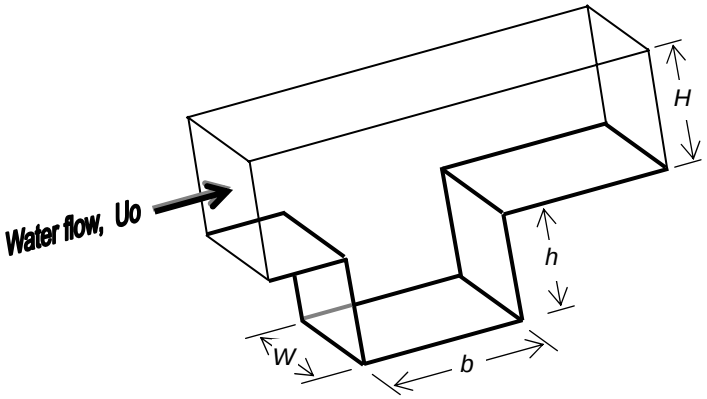

Figure 2: Open cavity geometric parameters.

Three different cavities have been used in the experimental runs, having aspect ratio of b/h = 1, 2, and 3, while the sizes W and H have been kept unchanged. For each case, four different Reynolds numbers have been adjusted, Re = 500, 700, 1000, and 1300. The Reynolds number is based on cavity depth (h) and average uniform velocity (Uo) at the channel inlet. The water flow rate has been determined using a previously calibrated orifice plate, with uncertainty of ±1%.

Two classical flow visualization procedures have been used in this work. Firstly, opaque liquid dye has been directly injected inside the cavity, with the help of an L-shape needle of 0.7 mm external diameter. Fluid flow images have been captured during dye wash process. A mix of PVA pigments, ethylic alcohol, and water, having viscosity and density nearly to the tap water, has been used as dye tracer. Diffuse back-light illumination has been necessary in order to produce sharp images with high contrast.

Secondly, solid micro-particles mixed in the flow have been used. In contrast with the precedent case, a light-sheet system is generally necessary to illuminate the region in the flow to be researched. In the most of time, that light-sheet is produced by an expanding laser beam through a cylindrical lens or due to the projection of the beam on a rotating hexagonal mirror. When illuminated by a thin light-sheet, small particles suspended in the flow produce scattering of incident light and become sharply visible. In the image capture process, sufficiently long exposition times will result into streaks of the particles on the plane image. Obviously, in steady-state flows streamlines and pathlines can also be observed, since in that case they are coincident with streaklines.

In this work, the light-sheet was generated by the in-house system illustrated in Fig. 3(a), in which the laser source has been replaced by a Kodak™ carrousel slide projector. To prevent undesirable luminosity entrance in the test section, the runs have been carried out in the nocturnal period and all the experimental apparatus, including the still camera, was covered by a black canvas, as showed in Fig. 3(b). For obtaining the negative slide showed in Fig. 3(c), a white paper containing a single black straight line was photographed using black & white graphics negative film. So, the dark line on the white paper appears as a transparent line on the negative slide. When inserted in the slide projector, only that transparent line will allow light passing, generating a leaf illuminated in the flow.

(a) Experimental apparatus (b) Opaque black cover (c) Negative high contrast slide

Figure 3: Experimental apparatus and in-house light-sheet generator system for flow visualization.

Pliolight™ micro-particles had been used as solid tracers. Photographs have been taken with a still digital camera Fuji™ FinePix S7000, of 6.0 Megapixels and 6x optical zoom. Many preliminary tests have been necessary in order to find the ideal exposition time to be adopted for each Reynolds number. To allow visual access to the flow and to facilitate framing and manual focalization operations, a high resolution monitor of 10" JVC™ CRT has been connected to the camera.

3. RESULTS AND DISCUSSION

Figure 4 presents flow patterns inside the cavity with $b/h = 1$, visualized with the help of solid micro-particles mixed into the water, while Fig. 5 presents images of the same flow obtained by liquid dye injection. As it can be observed, sharper images can be obtained using solid tracers, which allow accurately locating vortex kernels.

Figures 4(a) and 5(a) allow to observe that, for $Re = 500$, the separated shear layer rolls up into vortices and an elongated eddy structure fills all the superior part of the cavity. The kernel of that triangular vortex is situated near the right superior wall, close to the cavity outlet, and the fluid in cavity bottom remains practically stagnant.

For Reynolds number above 500, a large swirl having approximately the same cavity size is formed and the flow configuration is similar to that found in a lid-driven cavity. The kernel of that recirculation displaces toward the cavity center as Re increases from 700 to 1300. At the same time, two secondary eddies can be identified in both inferior corners of the cavity, which improve their circulation intensity as the Reynolds augment.

In Fig. 6, results obtained for $Re = 1300$ are confronted with numerical simulation from Frigo (2004), performed at $Re = 2648$. In spite of the Reynolds number not to be the same, these qualitative results present an excellent agreement. Indeed the arrows (1) and (2) in Fig. 6(a) point the experimental corner recirculation zones identified at $Re = 1300$, which present the same shape and size of those numerically calculated by Frigo (2004). Moreover, the circle indicated by the arrow (3) shows a streamlines deflection, which has been very well predicted by Frigo (2004).

Figure 7 presents images of the flow in an open cavity with aspect ratio $b/h = 2$, for different Reynolds numbers, obtained by using solid tracers. For this aspect ratio, the interaction of the internal flow and the free-stream in the canal above the cavity become more evident, when compared with the square cavity ($b/h = 1$). Besides, the large swirl observed at $b/h = 1$ is replaced by two contra-rotating eddies having a characteristic size of h.

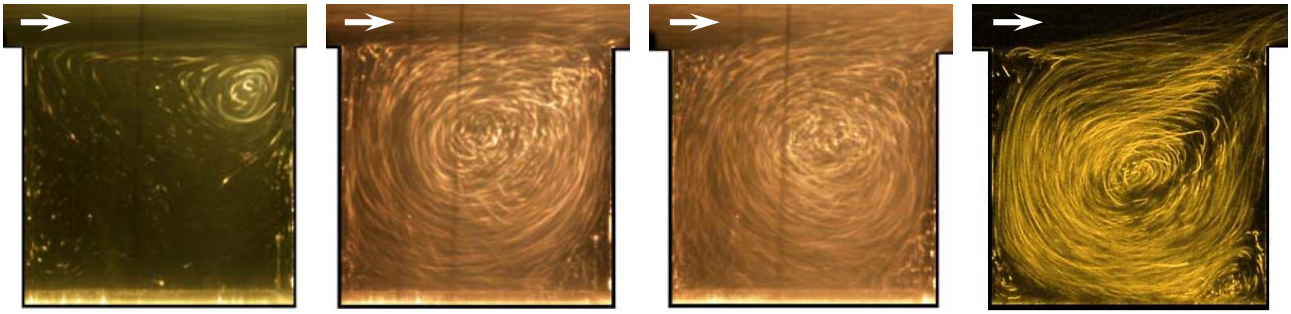

(a) Re = 500 (b) Re = 700 (c) Re = 1000 (d) Re = 1300

Figure 4: Flow inside the cavity with b/h = 1 visualized with the help of solid tracers.

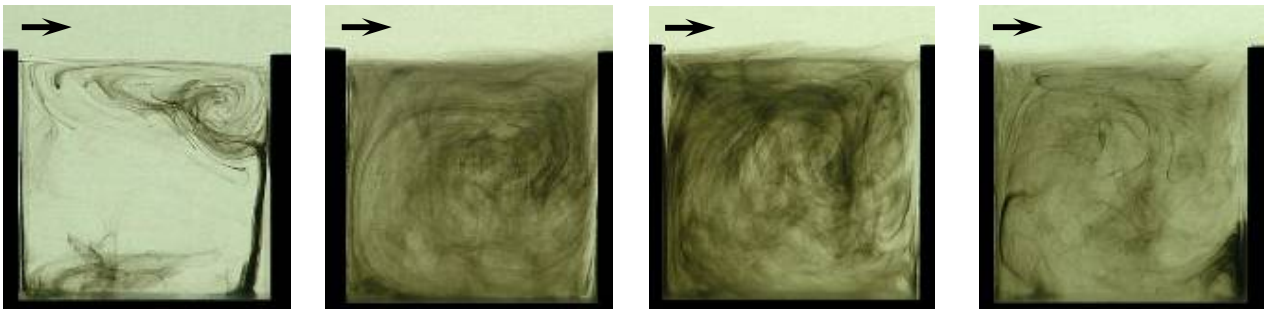

(a) Re = 500 (b) Re = 700 (c) Re = 1000 (d) Re = 1300

Figure 5: Flow inside the cavity with b/h = 1 visualized with the help of liquid dye injection.

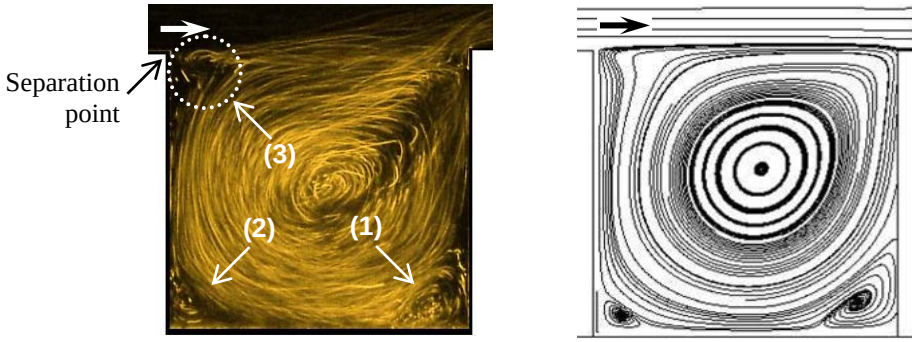

(a) Present work, Re = 1300 (b) Frigo (2004), Re = 2648

Figure 6: Flow inside the cavity with b/h = 1 – experimental and numerical results.

For comparison purpose, Fig. 8 shows the same flows visualized by means of the two techniques – dye injection and solid tracers. Using liquid dye injection flow visualization technique, the size and the kernel position of the vortical structures are not so evident. On the other hand, solid micro-particles illuminated by light-sheet does not allow identifying Kelvin-Helmholtz instabilities generated in the horizontal shear zone that connects the flows inside and outside the cavity. Physically, boundary layer separation occurs on the superior left edge of the cavity and Kelvin-Helmholtz instabilities arise and are advected, as a consequence of the pronounced inflexional velocity profile that characterizes such a flow.

Figure 9 allow again confronting experimental flow visualization obtained in this work with numerical simulation of Frigo (2004). The two main contra-rotating structures identified in the experimental results are well represented in the calculated streamlines map. Nevertheless, the two small recirculating bubbles observed in the inferior corners of the cavity in Fig. 9(b) are hardly visible in Fig. 9(a).

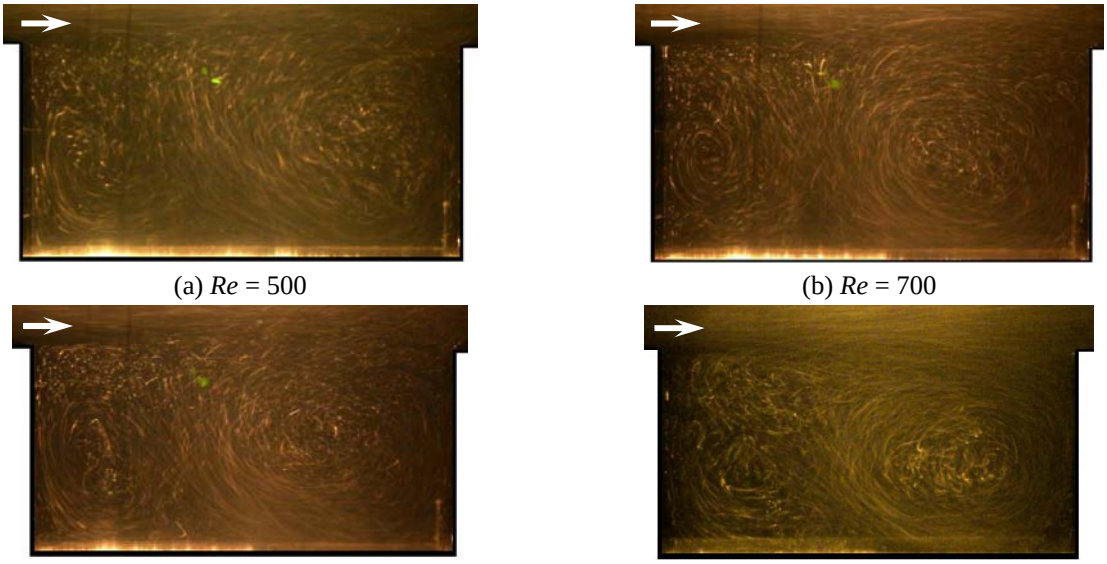

(a) *Re* = 500 (b) *Re* = 700

(c) *Re* = 1000 (d) *Re* = 1300

Figure 7: Flow inside the cavity with *b*/*h* = 2 visualized with the help of solid tracers.

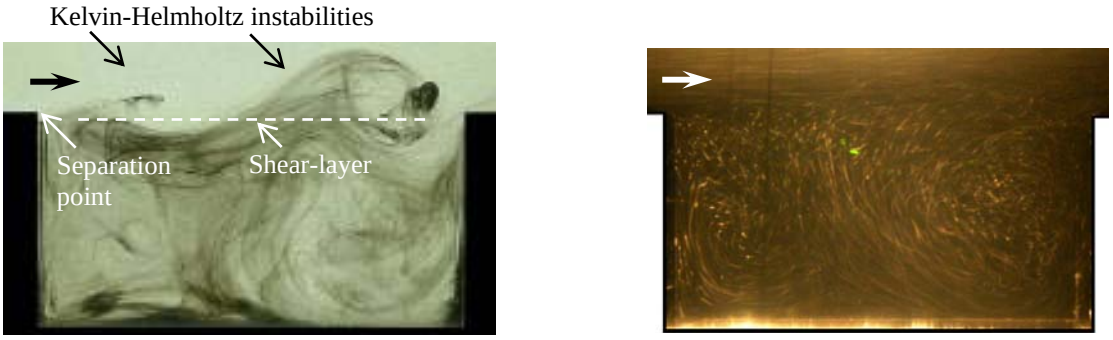

(a) liquid dye injection (b) Solid micro-particles tracers

Figure 8: Flow inside the cavity with *b*/*h* = 2 visualized by means of dye injection and solid tracers, at *Re*=500.

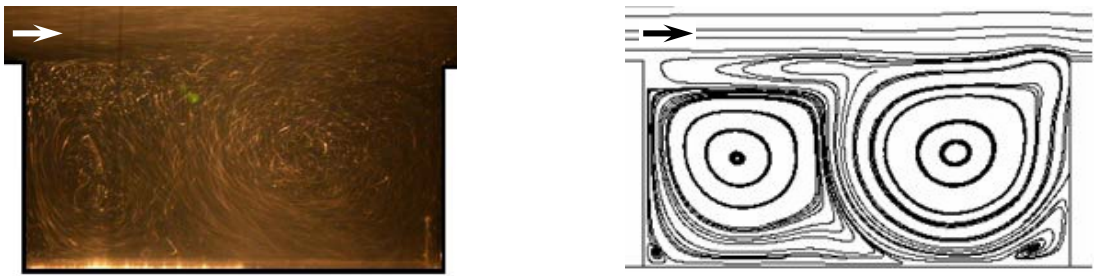

(a) Present work, *Re* = 1000 (b) Frigo (2004), *Re* = 2648

Figure 9: Flow inside the cavity with *b*/*h* = 2 – experimental and numerical results.

Figure 10 presents flow patterns corresponding to an open cavity with *b*/*h* = 3, at different Reynolds numbers, obtained by using solid tracers. As it has been observed in the precedent tests, the flow inside cavity seems divided in two halves occupying the left and the right sides of the cavity. Nevertheless, at the present case only the right half flow appears recirculating. The traces stamped by solid particles in the left half indicate the probable existence of a left-to-right oscillating fluid motion in that region. A more deepened investigation on that flow pattern is needed to bring insight on the subject, since studies concerning with shallow cavities at low Reynolds numbers are not abundant in the literature.

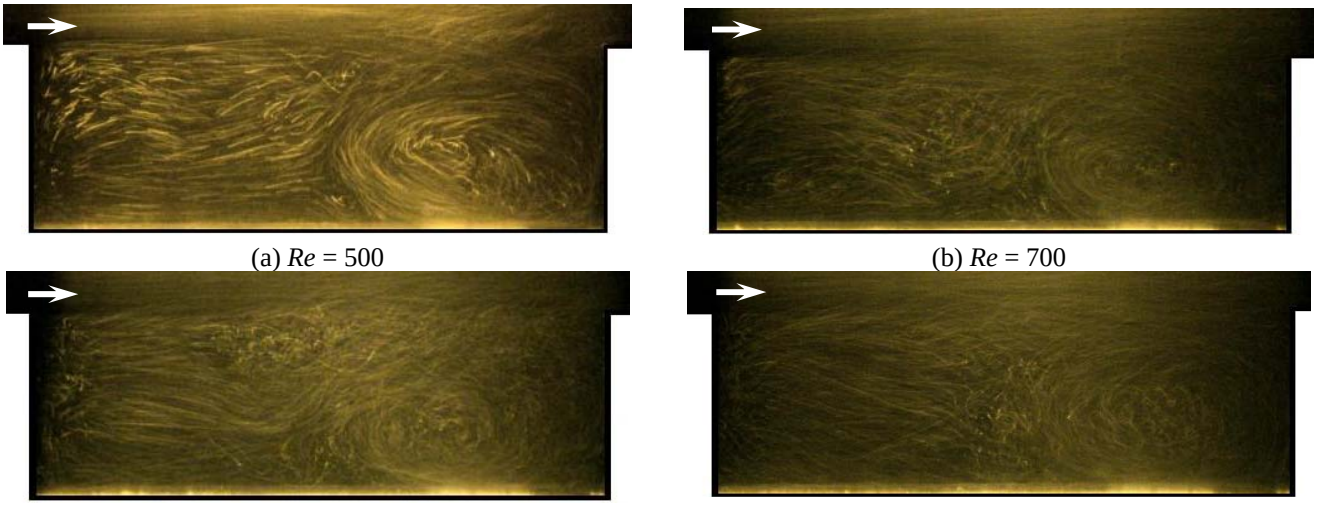

(a) *Re* = 500 (b) *Re* = 700

(c) *Re* = 1000 (d) *Re* = 1300

Figure 10: Flow inside the cavity with *b*/*h* = 3 visualized with the help of solid tracers.

Figure 11 shows the flow configurations obtained for the same cavity with *b*/*h* = 3 at *Re* = 700, using the two visualizations techniques. Once again, the use of solid tracers is inadequate to identify non-stationary vortical structures like Kelvin-Helmholtz instabilities formed in the cavity shear-layer. In that context, liquid dye injection supplies results considerably better.

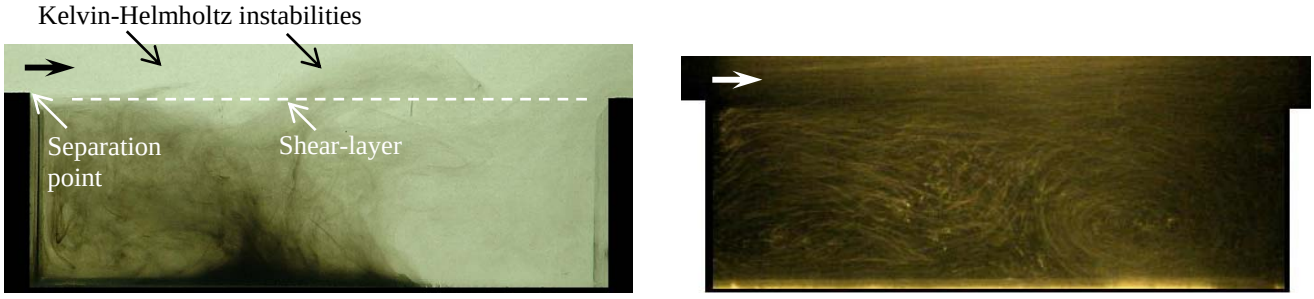

(a) Liquid dye injection (b) Solid micro-particles tracers

Figure 11: Flow inside the cavity with *b*/*h* = 3 visualized by means of dye injection and solid tracers, at *Re*=700.

4. CONCLUSION

In the present work, flow patterns inside open cavities have been qualitatively investigated, for different aspect ratios and different Reynolds numbers. Two classical flow visualizations techniques have been employed in the experimental tests, i.e., liquid dye injection and solid tracers.

In spite the geometrical simplicity of that problem, cavity flows can became very complex, presenting stationary recirculation, shear-layer instabilities, periodic eddies, and other secondary vortical structures that continuously interact among themselves. The flow patterns depends strongly on the intensity of these interactions and can change considerably with aspect ratio and Reynolds number.

The two flow visualization techniques have been satisfactorily employed for providing different insights. In a general way, solid micro-particles suspended in the fluid flow illuminated by light sheet produce good-quality images, which allow sharply identifying stationary vortical structures. On the other hand, liquid dye injection is more appropriate to identify inherent moving instability of the shear layer past the cavity.

5. ACKNOWLEDGEMENTS

The authors are grateful to FAPESP for the financial support.

6. REFERENCES

Colonius, T., Basu, A.J., Rowley, C.W., Numerical investigation of the flow past a cavity, *in*: Proc. 5th AIAA/CEAS Aeroacustics Conference, Greater Seattle, Washington, USA, 1999a.

Colonius, T., Basu, A.J., Rowley, C.W., Computation of sound generation and flow/acoustic instabilities in the flow past an open cavity, *in*: Proc. 3rd ASME/JSME Joint Fluids Engineering Conference, San Francisco, USA, 1999b.

Esteve, M.J., Reulet, P., Millan, P., Flow field characterization within a rectangular cavity, *in*: Proc. 10th International Symposium on Applications of Laser Techniques to Fluid Mechanics, Lisbon, Portugal, 2000.

Ludovic, B., Orkwis, P., Turner, M., Modeling unsteady cavity flows with translating walls, *in*: Proc. 32nd AIAA Fluid Dynamics Conference and Exhibit, St. Louis, USA, 2002.

Hamed, A., Basu, D., and Das, K., Detached eddy simulations of supersonic flow over cavity, *in*: Proc.41st AIAA Aerospace Sciences Meeting and Exhibit, AIAA-2003-0549, Reno, USA, 2003.

Frigo, L.M., Simulação Numérica de Escoamentos Incompressíveis Tridimensionais Turbulentos e em Transição, M.Sc. Dissertation, UNESP Ilha Solteira, Ilha Solteira, Brazil, 2004.

Gloerfelt, X., Bailly, C., Juvé, D., Simulation des grandes échelles du champ acoustique produit par un écoulement affleurant une cavité, *in*: Proc. 6ème Congrès Français d'Acoustique, pp.133-136, Lille, France, 2002.

Gloerfelt, X., Bailly, C., Juvé, D., Direct computation of the noise radiated by a subsonic cavity flow and application of integral methods, Journal of Sound and Vibration, v.266, pp.119-146, 2003a.

Gloerfelt, X., Bogey, C., Bailly, C., Numerical of mode switching in the flow-induced oscillations by a cavity, International Journal of Aeroacoustics, v.2, pp.99-124, 2003b.

Henderson, J., Badcock, K.J., Richards, B.E., Understanding subsonic and transonic cavity flows, The Aeronautical Journal, v.105, pp.77-84, 2001.

Kim, J.J., Baik, J.J., Chun, H.Y., Two-dimensional numerical modeling of flow and dispersion in the presence of hill and buildings, Journal of Wind Engineering and Industrial Aerodynamics, v.89, pp.947-966, 2001.

Lima e Silva, A.L.F., Damasceno, J.J.R., Silveira-Neto, A, Numerical simulation of two dimensional flows over a circular cylinder using the immersed boundary method, Journal of Computational Physics, v.189, pp.351-370, 2003

Reulet, P., Esteve, M.J., Millan, P., Riethmuller, M.L., Experimental characterization of the flow within a transitional rectangular cavity, Journal of Flow Visualization and Image Processing, v.9, pp.153-170, 2002.

Samimy, M., Debiasi, M., Caraballo, E., Özbay, H., Efe, M.Ö., Yuan, X., DeBonis, J., Myatt, J.H., Development of closed-loop control for cavity flows, *in*: Proc. 33rd AIAA Fluid Dynamics Conference and Exhibit, Orlando, USA, 2003.

Shen, C., Floryan, J.M, Low Reynolds number flow over cavities, Physics of Fluids, v.28, pp.3191-3202, 1985.

Sinha, S. N, Gupta, A.K., Oberai, M.M., Laminar separating flow over backsteps and cavities. Part II: Cavities, AIAA Journal, v.20, pp.370-375,1982.

Zdanski, P.S.B., Ortega, M.A., Fico Jr., N.G.C.R., Numerical simulation of laminar flow over shallow cavities, *in:* Proc. 8th Brazilian Congress of Engineering and Thermal Sciences – ENCIT, Porto Alegre, Brazil, 2000.

Zdanski, P.S.B., Ortega, M.A., Fico Jr., N.G.C.R., Numerical simulation of turbulent flow over shallow cavities, *in:* Proc. 2nd International Conference on Computational Heat and Mass Transfer, Rio de Janeiro, Brazil, 2001.

Zdanski, P.S.B., Ortega, M.A., Fico Jr., N.G.C.R., Numerical study of the flow over shallow cavities, Computers & Fluids, v.32, pp.953-974, 2003.

7. RESPONSIBILITY NOTICE

The authors are the only responsible for the printed material included in this paper.